Anisotropic Molecular Polarizabilities of HCHO, CH_3CHO, and CH_3COCH_3. Rayleigh Depolarization Ratios of HCHO and CH_3CHO and First and Second Kerr Virial Coefficients of CH_3COCH_3

Vincent W. Couling,[1a] Brendan W. Halliburton,[1b] Roland I. Keir,[1b] and Geoffrey L. D. Ritchie*,[1b]

School of Chemical and Physical Sciences, University of Natal, Pietermaritzburg 3209, South Africa, and Chemistry, School of Physical Sciences and Engineering, University of New England, Armidale, NSW 2351, Australia

Received: December 7, 2000; In Final Form: February 14, 2001

Available information in relation to the anisotropic electric dipole polarizabilities of HCHO, CH_3CHO, and CH_3COCH_3 is complemented by measurements of the vapor-phase Rayleigh depolarization ratios of HCHO and CH_3CHO and the temperature dependence of the vapor-phase electrooptical Kerr effect of CH_3COCH_3 at 632.8 nm. In the cases of HCHO and CH_3CHO the polarizabilities remain incompletely defined by the experimental data; but in the case of CH_3COCH_3 the three principal polarizabilities are determinable from an analysis of the Kerr effect together with the previously reported mean polarizability and Rayleigh depolarization ratio of this species. The experimental polarizabilities of CH_3COCH_3, in conjunction with Rice and Handy's computed polarizabilities of HCHO and a simple group additivity model, allow the reliable prediction of the four components of the polarizability of CH_3CHO. As well, the temperature dependence of the first Kerr virial coefficient of CH_3COCH_3 provides uncertain estimates of the first and second Kerr hyperpolarizabilities, which have not previously been reported. The temperature dependence of the second Kerr virial coefficient, which measures contributions from pairwise molecular interactions, is found to be explicable in terms of a recent statistical-mechanical theory of the effect.

Introduction

The electric dipole polarizability, $\alpha_{\alpha\beta}$, is the basic descriptor of the interaction of the molecular charge distribution with an electric field.[2−4] Although the principal polarizabilities of a useful number (<20) and variety of asymmetric tops (i.e., $\alpha_{xx} \neq \alpha_{yy} \neq \alpha_{zz}$) have now been evaluated experimentally (e.g., H_2O,[5] SO_2,[6,7] $H_2C{=}CH_2$[8,9]), those of the simplest carbonyl compounds, of which HCHO, CH_3CHO, and CH_3COCH_3 are the prime examples, have not yet been so determined. In the present study, available information for HCHO, CH_3CHO, and CH_3COCH_3 is complemented by measurements of the vapor-phase Rayleigh depolarization ratios of HCHO and CH_3CHO and the temperature dependence of the vapor-phase electrooptical Kerr effect (i.e., A_K and B_K vs T) of CH_3COCH_3. In the cases of HCHO and CH_3CHO the polarizabilities are still incompletely defined by the data; but in the case of CH_3COCH_3 the three principal polarizabilities are determinable by simultaneous solution of the three independent equations that arise from the newly measured temperature dependence of the first Kerr virial coefficient, A_K, together with the known mean polarizability, α, and Rayleigh depolarization ratio, ρ_0, of this species. The experimental polarizabilities of CH_3COCH_3, in combination with state-of-the-art computed polarizabilities of HCHO[10] and a simple group-additivity model, then allow the reliable prediction of the (four) components of the polarizability of CH_3CHO. It is found that the computed polarizabilities of HCHO, the group-additivity derived polarizabilities of CH_3CHO, and, of course, the experimental polarizabilities of CH_3COCH_3 accurately reproduce the observed mean polarizabilities and polarizability anisotropies of these three species, an excellent demonstration of the reliability of the results. As well, the temperature dependence of the first Kerr virial coefficient of CH_3COCH_3 yields poorly determined values of the first and second Kerr hyperpolarizabilities, β^K and γ^K, which have not previously been reported for this molecule. The temperature dependence of the second Kerr virial coefficient, B_K, which measures contributions to the observed effect from pairwise molecular interactions, is found to be explicable in terms of a recent generalization[11,12] of a statistical-mechanical theory based on the dipole−induced dipole model.[13]

Theory

Necessary theory has been given elsewhere,[7,11,14] and only a brief summary is included here. Note, too, that the reference axes for the polarizability, shown in Figure 1, are defined such that y and z are in the heavy-atom plane, with z coincident with the O═C bond; x is perpendicular to the heavy-atom plane. In the cases of HCHO and CH_3COCH_3 these reference axes are, in fact, the principal axes, but in the case of CH_3CHO this is not so; x remains a principal axis but y and z must be rotated through an angle θ in the yz plane to locate the principal axes.

The relationship between the Rayleigh depolarization ratio $\rho_0 = I_h^v/I_v^v$ and the optical-frequency polarizability is[14]

$$5\rho_0(3 - 4\rho_0)^{-1} = \kappa^2 = (3\alpha_{\alpha\beta}\alpha_{\alpha\beta} - \alpha_{\alpha\alpha}\alpha_{\beta\beta})(2\alpha_{\alpha\alpha}\alpha_{\beta\beta})^{-1} \quad (1)$$

in which κ is the polarizability anisotropy parameter and

* To whom correspondence should be addressed.

10.1021/jp0044173 CCC: $20.00
Published on Web 04/11/2001

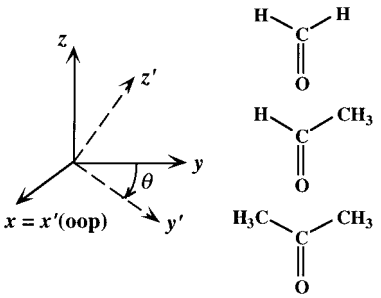

Figure 1. Definition of axes (oop = out-of-plane): x, y, z = principal axes for HCHO and CH_3COCH_3 and reference axes for CH_3CHO; x', y', z' = principal axes for CH_3CHO.

$$\alpha_{\alpha\alpha}/3 = \alpha = (\alpha_{xx} + \alpha_{yy} + \alpha_{zz})/3 \quad (2)$$

is the mean polarizability. The expressions for κ^2 in terms of the components of the polarizability in the reference axis system are

$$\kappa^2 = [(\alpha_{xx} - \alpha_{yy})^2 + (\alpha_{yy} - \alpha_{zz})^2 + (\alpha_{zz} - \alpha_{xx})^2]/18\alpha^2 \quad (3)$$

for HCHO and CH_3COCH_3 (where the reference and principal axes coincide) and

$$\kappa^2 = [(\alpha_{xx} - \alpha_{yy})^2 + (\alpha_{yy} - \alpha_{zz})^2 + (\alpha_{zz} - \alpha_{xx})^2 + 6\alpha_{yz}{}^2]/18\alpha^2 \quad (4)$$

for CH_3CHO (where the reference and principal axes do not coincide). In the case of CH_3CHO there are, therefore, four, not three, components of the polarizability to be evaluated in the reference axis system.

The definition of the molar Kerr constant, ${}_mK$, is[15−17]

$${}_mK = 6nV_m[(n^2 + 2)^2(\epsilon_r + 2)^2]^{-1}[(n_X - n_Y)/F_X{}^2]_{F_X = 0} \quad (5)$$

where n and ϵ_r are the refractive index and relative permittivity of the gas in the absence of the field, $n_X - n_Y$ is the birefringence for XZ and YZ polarized light that is induced by the uniform electric field, F_X, and V_m is the molar volume. To take account of molecular interactions, ${}_mK$ can be expressed in terms of V_m as

$${}_mK = A_K + B_K V_m{}^{-1} + ... \quad (6)$$

in which A_K and B_K are the first and second Kerr virial coefficients; A_K is the zero-density value of ${}_mK$, and B_K measures the additional contribution to ${}_mK$ from interacting pairs of molecules. The first Kerr virial coefficient of CH_3COCH_3 is, in SI units[7,16,17]

$$A_K = (N_A/81\epsilon_0)\{\gamma^K + (kT)^{-1}[(2/3)\mu\beta^K + (9/5)\alpha\alpha^0\kappa\kappa^0] + (3/10)(kT)^{-2}\mu^2(\alpha_{zz} - \alpha)\} \quad (7a)$$

$$= P + QT^{-1} + RT^{-2} \quad (7b)$$

where eq 7a relates A_K to molecular properties and eq 7b emphasizes the quadratic dependence of A_K on T^{-1}. As well, μ is the molecular dipole moment, α and α^0 are the mean optical-frequency and static polarizabilities, α_{zz} is the component of $\alpha_{\alpha\beta}$ in the direction (− to +) of μ, $\kappa\kappa^0$ ($\approx\kappa^2$) is the product of the optical-frequency and static polarizability anisotropy parameters,[7] and β^K and γ^K are the first and second Kerr hyperpolarizabilities.[2] The coefficients P, Q, and R are

$$P = (N_A/81\epsilon_0)\gamma^K \quad (8)$$

$$Q = (N_A/81\epsilon_0 k)[(2/3)\mu\beta^K + (9/5)\alpha\alpha^0\kappa\kappa^0] \quad (9)$$

$$R = (N_A/81\epsilon_0 k^2)(3/10)\mu^2(\alpha_{zz} - \alpha) \quad (10)$$

so that P and Q give γ^K and β^K, respectively, and R gives the desired equation in α_{xx}, α_{yy}, and α_{zz}.

The second Kerr virial coefficient, B_K, is[11]

$$B_K = (N_A{}^2/54\Omega\epsilon_0)\int_\tau (\alpha_2 + \alpha_3 + \alpha_4 + ... + \mu_2\alpha_1 + \mu_2\alpha_2 + \mu_2\alpha_3 + ...) \exp(-U_{12}(\tau)/kT)\, d\tau \quad (11)$$

where $\Omega = V_m{}^{-1} \int_\tau d\tau$ is the integral over the orientational coordinates of the neighboring molecule, α_2, α_3, α_4, ... are terms in powers of the optical-frequency and static polarizabilities that result from partial orientation of anisotropic pairs, $\mu_2\alpha_1$, $\mu_2\alpha_2$, $\mu_2\alpha_3$, ... result from partial orientation of the coupled dipole moments of pairs, and $U_{12}(\tau)$ is the intermolecular pair potential energy. As previously,[11,12] $U_{12}(\tau)$ is expressed as

$$U_{12}(\tau) = U_{LJ} + U_{\mu\mu} + U_{\mu\Theta} + U_{\Theta\Theta} + U_{\mu\mathrm{ind}\mu} + U_{\Theta\mathrm{ind}\mu} + U_{\mathrm{shape}} \quad (12)$$

in which U_{LJ} is the Lennard-Jones 6:12 potential, $U_{\mu\mu}$, $U_{\mu\Theta}$, and $U_{\Theta\Theta}$ are the dipole−dipole, dipole−quadrupole, and quadrupole−quadrupole interaction energies, $U_{\mu\mathrm{ind}\mu}$ and $U_{\Theta\mathrm{ind}\mu}$ are the dipole-induced dipole and quadrupole-induced dipole interaction energies, and U_{shape} accounts for the angular dependence of short-range repulsive forces for nonspherical molecules. General expressions, applicable to nonlinear species such as CH_3COCH_3, for the terms in eqs 11 and 12 have been given elsewhere.[11]

Experimental Section

Samples were prepared as follows: Formaldehyde (Aldrich, 37% by mass in water, stabilized by 10−15% methanol) was treated by a variant of the standard procedure.[18] The gas (bp −21 °C) is susceptible to polymerization, and the scattering cell was maintained at an elevated temperature (97.5 °C) to minimize deposition of polymeric species. Acetaldehyde (Aldrich, >99%, bp 20 °C) was subjected to two freeze−pump−thaw cycles, which included vacuum distillation, immediately before introduction into the scattering cell. Acetone (99%, bp 56 °C) was distilled three times through a 1.2 m packed column and dried over 0.4 nm molecular sieves; gas-chromatographic analysis gave the purity of the sample as >99.99%.

Improved apparatus for measurements of the Rayleigh depolarization ratio, $\rho_0 = (I_h^v - I_{h,b}^v)/(I_v^v - I_{v,b}^v)$, of gases and vapors at 632.8 nm has been described.[19] Observations on HCHO were made at 97.5 °C and ≈26 kPa; those on CH_3CHO were made at 25 °C and ≈40 kPa. Typical count rates (counts/s) for the depolarized and polarized signals, I_h^v and I_v^v, and the backgrounds, $I_{h,b}^v$ and $I_{v,b}^v$, were the following: HCHO, 22, 1214, 8, 15; CH_3CHO, 140, 16 494, 5.4, 25. Integration times were in the range 100−800 s. The results are the averages of repeated determinations, ≈5 with inclusion and ≈5 with exclusion by means of an interference filter of vibrational Raman contributions: HCHO, $\rho_0 = (1.41 \pm 0.14) \times 10^{-2}$ (inclusion), $(1.23 \pm 0.09) \times 10^{-2}$ (exclusion); CH_3CHO, $\rho_0 = (0.815 \pm 0.004) \times 10^{-2}$ (inclusion), $(0.77 \pm 0.03) \times 10^{-2}$ (exclusion). Clearly, the precision of the results for HCHO is far below what

TABLE 1: Temperature Dependence of the Vapor-State Kerr Effect of CH_3COCH_3 at 632.8 nm

T (K)	no. of pressures	p (kPa)	B^a (10^{-6} m^3 mol^{-1})	A_K (10^{-27} m^5 V^{-2} mol^{-1})	B_K (10^{-29} m^8 V^{-2} mol^{-2})
489.8	9	38−90	−331	34.9 ± 0.3	1 ± 1
479.3	8	32−89	−383	36.9 ± 0.4	−1 ± 2
456.8	10	32−87	−429	40.0 ± 0.2	2 ± 1
423.8	9	32−78	−486	47.1 ± 0.4	2 ± 2
404.8	9	31−74	−588	51.2 ± 0.4	7 ± 2
383.8	9	33−73	−750	57.0± 0.2	5 ± 1
370.4	10	21−65	−881	61.4 ± 0.4	8 ± 2
350.9	8	21−58	−1106	69.4 ± 0.7	4 ± 4
330.8	10	15−60	−1385	76.5 ± 0.7	19 ± 4
315.7	9	15−64	−1613	85.8 ± 0.7	10 ± 4
308.5	9	14−44	−1772	89.7 ± 0.1	21 ± 2
298.2	9	8−30	−2033	95.5 ± 0.6	23 ± 6

[a] Pressure second virial coefficients from ref 24.

is typically achieved, presumably as a consequence of polymerization. In the discussion that follows, the higher depolarization ratios (i.e., those that include vibrational Raman contributions) are preferred for HCHO and CH_3CHO, at least partly for consistency with CH_3COCH_3;[20] but the conclusions in respect of HCHO and CH_3CHO would be effectively the same if the alternatives were used.

Equipment and procedures for investigations of the temperature and pressure dependence of the electrooptical Kerr effect in gases and vapors have also been described.[7,21] Measurements of the field-induced birefringence of CH_3COCH_3 were made at 12 temperatures (≈298−490 K) within the available span and, at each temperature, over a range of pressures (≈8−90 kPa). The observed birefringences of the gas were used to establish values of ${}_mK_0 = (2/27)V_m(n_X - n_Y)/F_X{}^2$, and these were fitted to the relation[22]

$$ {}_mK_0 = A_K + \left[B_K + A_K\left(2A_\epsilon + \frac{1}{2}A_R\right)\right]V_m{}^{-1} \qquad (13) $$

in which A_ϵ and A_R are the low-density molar dielectric polarization[23] and refraction, the latter calculated from the optical-frequency molecular polarizability.[20] Pressure virial coefficients, B,[24] were used to obtain molar volumes, V_m, from the vapor temperatures and pressures. The results are summarized in Table 1, where the errors attributed to the values of A_K are standard deviations obtained from the least-squares fitting of straight lines to the density-dependence data; with calibration and other systematic errors the overall accuracy is estimated as ±2%. Despite the relatively low pressures at which the measurements were performed, acceptably precise values of B_K have also been derived.

The vapor-phase Kerr effect of CH_3COCH_3 was first examined more than 70 years ago: a single-temperature measurement by Stuart[25] yielded a bulk Kerr constant, K, at 356.2 K and 101.3 kPa of 31.2×10^{-15} esu, which corresponds to a molar Kerr constant, ${}_mK$, of ≈72.4×10^{-27} m^5 V^{-2} mol^{-1}, at 589 nm. By comparison, interpolation from the present measurements indicates a value, at 356.2 K and 101.3 kPa, of ≈70.0×10^{-27} m^5 V^{-2} mol^{-1} at 632.8 nm or, with a correction for the wavelength dependence of the polarizability anisotropy, ≈72.0×10^{-27} m^5 V^{-2} mol^{-1} at 589 nm. In the context of the available technology, the earlier measurements, even if performed at only one temperature, were a remarkable achievement. Unfortunately, however, the theory of the Kerr effect was, at the time, incompletely understood, and the necessity for extensive measurements of the temperature dependence was not appreciated.

Results and Discussion

Temperature Dependence of A_K for CH_3COCH_3. The procedure was as previously described:[7] Figure 2 displays the experimental data and the fitted plot of A_K against T^{-1}; Table 2 contains the coefficients P, Q, and R of the polynomial $A_K = P + QT^{-1} + RT^{-2}$, together with the interpretation of these in terms of molecular properties. Other data in Table 2 are the mean optical-frequency[20] and static[23] polarizabilities, α and α^0, the square of the optical-frequency polarizability anisotropy

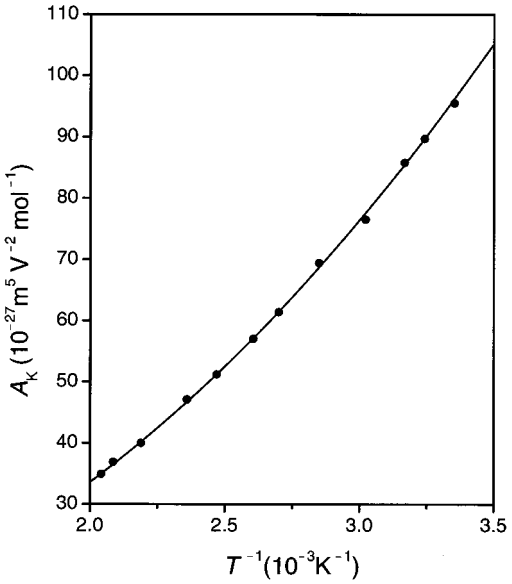

Figure 2. Temperature dependence of A_K of CH_3COCH_3.

TABLE 2: Analysis of the Temperature Dependence of A_K of CH_3COCH_3 at 632.8 nm

property	value
P (10^{-27} m^5 V^{-2} mol^{-1})[a]	8.4 ± 4.0
Q (10^{-24} m^5 V^{-2} mol^{-1} K)[a]	−7.5 ± 3.0
R (10^{-21} m^5 V^{-2} mol^{-1} K^2)[a]	10.06 ± 0.56
γ^K (10^{-60} C m^4 V^{-3})	10 ± 5[b]
α (10^{-40} C m^2 V^{-1})	7.14 ± 0.04[c]
α^0 (10^{-40} C m^2 V^{-1})	8.1 ± 0.7[d]
κ^2 (10^{-2})	0.890 ± 0.008[c]
μ (10^{-30} C m)	9.64 ± 0.07[d]
β^K (10^{-50} C m^3 V^{-2})	−2 ± 1[b]
α_{xx}(10^{-40} C m^2 V^{-1})[e]	5.80 ± 0.13[f] (7.66 ± 0.17)[g]
α_{yy}	7.66 ± 0.17[f] (5.80 ± 0.13)[g]
α_{zz}	7.96 ± 0.06

[a] See text; $A_K = P + QT^{-1} + RT^{-2}$. [b] For reasons noted in the text, γ^K and β^K are poorly determined in this analysis; the uncertainties shown are the apparent standard deviations, but both values are larger in magnitude than would be expected for a molecule of this size. [c] Reference 20. [d] Reference 23. [e] Locations of molecular axes: x perpendicular to heavy-atom plane; y and z in plane; z coincident with dipole moment (Figure 1). [f] Preferred values (see text). [g] Alternative solution of quadratic equation (see text).

TABLE 3: Contributions to A_K of CH_3COCH_3 at 300 and 500 K

term	value (10^{-27} m^5 V^{-2} mol^{-1}) 300 K	500 K
$(N_A/81\epsilon_0)\gamma^K$	8.4 (+8.9%)	8.4 (+25.1%)
$(2N_A/243\epsilon_0 kT)\mu\beta^K$	−27.0 (−28.4%)	−16.2 (−48.3%)
$(N_A/45\epsilon_0 kT)\alpha\alpha^0\kappa^2$	1.9 (+2.0%)	1.1 (+3.4%)
$(N_A/270\epsilon_0 k^2T^2)\mu^2(\alpha_{zz} - \alpha)$	111.8 (+117.6%)	40.2 (+119.8%)
A_K	95.1	33.6

parameter, $\kappa^2 = 5\rho_0(3 - 4\rho_0)^{-1}$,[20] and the molecular dipole moment, μ, obtained from the temperature dependence of the dielectric polarization.[23] The new results are the hyperpolarizabilities, γ^K and β^K, derived from eqs 8 and 9, and the components α_{xx}, α_{yy}, and α_{zz} of the optical-frequency molecular polarizability, derived by simultaneous solution of eqs 2, 3, and 10.

The absolute and percentage contributions of the four terms in eq 7a to the values of A_K at 300 and 500 K are shown in Table 3. Once again, the observed effect is strongly dominated by the $\mu^2(\alpha_{zz} - \alpha)$ term, with progressively smaller contributions from, in order, the $\mu\beta^K$, γ^K, and $\alpha\alpha^0\kappa^2$ terms. The consequence of this imbalance of terms, together with the demanding nature of the curve-fitting that is involved, is that the coefficients P and Q, and the derived hyperpolarizabilities γ^K and β^K, are imprecisely determined, whereas the coefficient R, and the polarizability anisotropy $\alpha_{zz} - \alpha$, are precisely determined by the measurements.

A matter of some subtlety in relation to the evaluation of the polarizabilities of CH_3COCH_3 is that simultaneous solution of eqs 2, 3, and 10, of which eq 3 is quadratic, yields two possible sets of polarizabilities that satisfy the equations. Fortunately, the choice between the alternatives was easily made on the basis of the magnetooptical Cotton−Mouton effect of CH_3COCH_3, which was also examined in this study. In fact, the Cotton−Mouton effect (the magnetic-field analogue of the Kerr effect) of gaseous CH_3COCH_3 was measured over a wide range of temperature, in the expectation that the data would provide an additional, independent, equation in the molecular polarizabilities.[26] In the event, however, the observed effect was too small to permit its temperature dependence to be specified with the precision that is required. Nevertheless, the effect was sufficiently well determined to resolve the present ambiguity. Over the temperature range noted above, the coefficient Q' which defines the temperature dependence of the Cotton−Mouton constant was found to be $Q' = (0.63 \pm 0.12) \times 10^{-24}$ m^5 A^{-2} mol^{-1} K, whereas the alternative sets of polarizabilities in Table 2, in conjunction with the known molecular magnetizabilities,[27] predict $Q' = (0.60 \pm 0.06) \times 10^{-24}$ m^5 A^{-2} mol^{-1} K and $Q' = (0.40 \pm 0.07) \times 10^{-24}$ m^5 A^{-2} mol^{-1} K, respectively. Clearly, the first set is correct and the second set, shown in parentheses, can be discarded. It can therefore be concluded that the anisotropic optical-frequency polarizability of CH_3COCH_3 is now well defined.

Anisotropic Polarizabilities of HCHO, CH_3CHO, and CH_3COCH_3. As noted above, the anisotropic molecular polarizability of HCHO remains incompletely defined by experiment and only two equations, eqs 2 and 3, in the three unknowns α_{xx}, α_{yy}, and α_{zz}, are available. Fortunately, however, ab initio optical-frequency polarizabilities, obtained with large basis sets at the MP2 level of theory, have been reported for HCHO,[10] and these made possible a useful analysis of the polarizability in the series HCHO, CH_3CHO, and CH_3COCH_3. The procedure was (a), for HCHO, to demonstrate that the computed polarizabilities accurately reproduce the experimental values of the mean polarizability, α, and the polarizability anisotropy, $\Delta\alpha$, (b), for CH_3CHO, to combine the computed polarizabilities for HCHO and the experimental polarizabilities for CH_3COCH_3 to predict the four independent components of the polarizability, and (c), also for CH_3CHO, to demonstrate that the predicted polarizabilities again accurately reproduce the experimental values of α and $\Delta\alpha$.

For the purposes of this analysis, the polarizability anisotropy, $\Delta\alpha$, is defined by the relation

$$(\Delta\alpha)^2 = 9\alpha^2\kappa^2 = \frac{1}{2}(3\alpha_{\alpha\beta}\alpha_{\alpha\beta} - \alpha_{\alpha\alpha}\alpha_{\beta\beta}) \qquad (14)$$

so that in the cases of HCHO and CH_3COCH_3

$$|\Delta\alpha| = \frac{1}{\sqrt{2}}\{(\alpha_{xx} - \alpha_{yy})^2 + (\alpha_{yy} - \alpha_{zz})^2 + (\alpha_{zz} - \alpha_{xx})^2\}^{1/2} \qquad (15)$$

and in the case of CH_3CHO

$$|\Delta\alpha| = \frac{1}{\sqrt{2}}\{(\alpha_{xx} - \alpha_{yy})^2 + (\alpha_{yy} - \alpha_{zz})^2 + (\alpha_{zz} - \alpha_{xx})^2 + 6\alpha_{yz}^2\}^{1/2} \qquad (16)$$

where the symbols are as defined in eqs 1−4. As well, it seems reasonable to expect the polarizabilities of the structurally similar species HCHO, CH_3CHO, and CH_3COCH_3 to conform, at least approximately, to a simple group-additivity model with contributions from the CH_3–C, H−C, and C═O groups and the assumption of regular bond angles. On this basis, the four components of the polarizability of CH_3CHO can be written in terms of the computed polarizabilities of HCHO[10] and the experimental polarizabilities of CH_3COCH_3 as

$$\alpha_{xx}(CH_3CHO) = \frac{1}{2}\{\alpha_{xx}(HCHO) + \alpha_{xx}(CH_3COCH_3)\} \qquad (17)$$

$$\alpha_{yy}(CH_3CHO) = \frac{1}{2}\{\alpha_{yy}(HCHO) + \alpha_{yy}(CH_3COCH_3)\} \qquad (18)$$

$$\alpha_{zz}(CH_3CHO) = \frac{1}{2}\{\alpha_{zz}(HCHO) + \alpha_{zz}(CH_3COCH_3)\} \qquad (19)$$

$$\alpha_{yz}(CH_3CHO) = -\frac{\sqrt{3}}{4}\{(\alpha_{yy} - \alpha_{zz})(HCHO) - (\alpha_{yy} - \alpha_{zz})(CH_3COCH_3)\} \qquad (20)$$

where the reference axes are as defined in Figure 1 and the fact that α_{yz} is not zero reflects the lower symmetry of CH_3CHO in comparison with HCHO and CH_3COCH_3.

The analysis is shown in Table 4, from which several useful conclusions can be drawn. Obviously, the computed polarizabilities for HCHO do indeed accurately reproduce the experimental values of α and $\Delta\alpha$, and HCHO is an instance where theory presently outperforms experiment. As well, the predicted polarizabilities for CH_3CHO adequately reproduce the experimental values of α and $\Delta\alpha$ for this species and, despite the limitations of the model, these too can be considered reliable. In relation to CH_3CHO, it remains to diagonalize the polarizability tensor, i.e., to determine the angle θ (see Figure 1)

TABLE 4: Polarizabilities[a] of HCHO, CH_3CHO, and CH_3COCH_3

	value (10^{-40} C m^2 V^{-1})		
property	HCHO	CH_3CHO	CH_3COCH_3
α(exptl)	(2.94)[b]	5.08 ± 0.05[c] (5.03)[b]	7.14 ± 0.04[d] (7.12)[b]
$\lvert\Delta\alpha\rvert$(exptl)	1.37 ± 0.07[e]	1.79 ± 0.09[e]	2.02 ± 0.03[e]
α_{xx}	2.152[f]	3.98[g] (3.98)[h]	5.80 ± 0.13[i]
α_{yy}	2.989[f]	5.32[g] (5.26)[h]	7.66 ± 0.17[i]
α_{zz}	3.711[f]	5.84[g] (5.89)[h]	7.96 ± 0.06[i]
α_{yz}		0.181[g]	
α(calcd)	2.951[j]	5.05[j]	
$\lvert\Delta\alpha\rvert$(calcd)	1.358[k]	1.69[k]	

[a] Mean values (α), anisotropies ($|\Delta\alpha|$), and components (α_{xx}, α_{yy}, α_{zz}) at 632.8 nm. All values expressed in units of 10^{-40} C m^2 V^{-1}. Conversion factors: 1×10^{-40} C m^2 V^{-1} = 0.8988×10^{-24} cm^3 = 6.065 au. [b] Values in parentheses estimated from experimental bond refractions: Vogel, A. I.; Cresswell, W. T.; Jeffrey, G. H.; Leicester, J. *J. Chem. Soc.* **1952**, 514−549. [c] Estimated from liquid-state refractive index and density; $n_D^{20} = 1.3316$, $\rho_4^{18} = 0.7834$, $\alpha = (3\epsilon_0/N_A)[(n^2 - 1)/(n^2 + 2)](M/\rho)$. [d] Reference 20. [e] Equation 14; $|\Delta\alpha|$(exptl) = $3\alpha\kappa$. [f] Reference 10. [g] Equations 17−20; reference axis system. [h] Principal polarizabilities (see text). [i] Equations 2, 3, and 10. [j] α(calcd) = $(\alpha_{xx} + \alpha_{yy} + \alpha_{zz})/3$. [k] Equations 15 and 16.

through which the reference y and z axes must be rotated, about the x axis and in the yz plane, to locate the principal y and z axes, labeled y' and z'. From the transformation law for a second-rank tensor, and with the axes and sense of rotation shown in Figure 1, it is easily established that the connection between the polarizabilities in the reference axis system and the angle θ is

$$\tan 2\theta = 2\alpha_{yz}(\alpha_{zz} - \alpha_{yy})^{-1} \qquad (21)$$

from which θ emerges as 17.6°. Table 4, which also contains, in parentheses, the principal polarizabilities of CH_3CHO, therefore constitutes a reliable summary of the polarizabilities of HCHO, CH_3CHO, and CH_3COCH_3.

Temperature Dependence of B_K for CH_3COCH_3. As already noted, the second Kerr virial coefficient, B_K, measures contributions to the observed effect from pairwise interactions and it is, therefore, a useful source of information about the effective intermolecular pair potential energy function.[11,12] In the present work the procedure was to use optimized force constants and shape factors and the recently developed theory to calculate B_K over the relevant range of temperature and then to compare the theoretical and experimental results. The integrals in eq 11 were evaluated in the manner described;[11] program run times on a Silicon Graphics Origin 200 workstation with twin MIPS R10 000 processors and 256 Mb of memory were about 30 min. Optimized Lennard-Jones force constants, R_0 and ϵ/k, and shape factors, D_1 and D_2, for CH_3COCH_3 were obtained by fitting calculated values of the second pressure virial coefficient, $B(T)$, given by

$$B(T) = (N_A/2\Omega)\int_\tau [1 - \exp(-U_{12}(\tau)/kT)]\, d\tau \qquad (22)$$

to experimental data over the same range of temperature. The optimized parameters and other molecular properties used in the calculations of B_K are in Table 5, a comparison of the experimental and calculated values of $B(T)$ is in Table 6, and the contributions of the leading terms in eq 11 to the values of B_K at 300 and 500 K are in Table 7. At the higher temperature the dominant contribution to B_K arises from the $\mu_2\alpha_2$ term, with much smaller contributions from the $\mu_2\alpha_3$ and $\mu_2\alpha_4$ terms; the $\mu_2\alpha_5$ and higher-order collision-induced contributions can therefore be neglected.

TABLE 5: Molecular Properties for Calculations of B_K of CH_3COCH_3

property	value
R_0 (nm)	0.47[a]
ϵ/k (K)	360[a]
D_1	0.210 57[a]
D_2	0.231 93[a]
μ (10^{-30} C m)	9.64 ± 0.07[b]
Θ_{xx} (10^{-40} C m^2)	6.07 ± 0.50[c]
Θ_{yy}	9.24 ± 0.43[c]
Θ_{zz}	-15.31 ± 0.33[c]
α_{xx} (10^{-40} C m^2 V^{-1})	5.80 ± 0.13[d]
α_{yy}	7.66 ± 0.17[d]
α_{zz}	7.96 ± 0.06[d]
α	7.14 ± 0.04[e]
$\lvert\Delta\alpha\rvert$	2.02 ± 0.03[f]
α^0_{xx} (10^{-40} C m^2 V^{-1})	6.58[g]
α^0_{yy}	8.69[g]
α^0_{zz}	9.03[g]
α^0	8.1 ± 0.7[b]
$\lvert\Delta\alpha^0\rvert$	2.30[h]

[a] Optimized force constants, R_0 and ϵ/k, and shape factors, D_1 and D_2, obtained by fitting calculated pressure virial coefficients to experimental data over the appropriate range of temperature. [b] Reference 23. [c] Reference 27. [d] Optical-frequency (632.8 nm) polarizabilities from Table 4. [e] Reference 20. [f] $|\Delta\alpha| = 3\alpha\kappa$. [g] Static polarizabilities; in the absence of reported values, it is assumed that $\alpha^0_{xx} \approx (\alpha^0/\alpha)\alpha_{xx} = 1.13\alpha_{xx}$, etc. [h] Equation 15.

TABLE 6: Comparison of Experimental and Calculated Values of $B(T)$ of CH_3COCH_3

	$B(T)$ (10^{-6} m^3 mol^{-1})			$B(T)$ (10^{-6} m^3 mol^{-1})	
T(K)	exptl[a]	calcd[b]	T(K)	exptl[a]	calcd[b]
300	−2000	−2055.7	350	−1060	−1041.0
310	−1730	−1737.8	360	−960	−941.6
320	−1520	−1497.1	400	−700	−674.3
330	−1350	−1310.0	440	−490	−518.1
340	−1200	−1161.4	480	−380	−415.3

[a] Reference 24. [b] Equation 22.

TABLE 7: Contributions to B_K of CH_3COCH_3 at 300 and 500 K[a]

	value (10^{-30} m^8 V^{-2} mol^{-1})			value (10^{-30} m^8 V^{-2} mol^{-1})	
term	300 K	500 K	term	300 K	500 K
$\mu_2\alpha_1$	−256.15	−5.57	α_3	−4.21	−0.09
$\mu_2\alpha_2$	190.32	20.35	α_4	11.34	0.87
$\mu_2\alpha_3$	174.20	10.71	α_5	0.67	0.08
$\mu_2\alpha_4$	14.45	1.50	B_K	131.71	27.88
α_2	1.09	0.03			

[a] Equation 11; $R_0 = 0.47$ nm, $\epsilon/k = 360$ K, $D_1 = 0.210\,57$, and $D_2 = 0.231\,93$.

The satisfactory agreement between the calculated and experimental values of B_K is apparent from Figure 3. To investigate the sensitivity of B_K to the chosen value of ϵ/k, computations were performed with $\epsilon/k = 350-380$ K and $R_0 = 0.47$ nm, in each case with optimized values of D_1 and D_2; the variation in B_K was <5% at 300 K and <1% at 500 K. The sensitivity of B_K to the chosen value of R_0 was similarly explored, and typical results are included in Figure 3. It is immediately apparent that B_K is far less sensitive to changes in ϵ/k (with R_0 fixed) than it is to changes in R_0 (with ϵ/k fixed). Indeed, the sensitivity of B_K to R_0, especially at relatively low temperatures, is greater than that exhibited by the few other molecules previously examined, possibly because of the large dipole moment and highly anisotropic polarizability of this

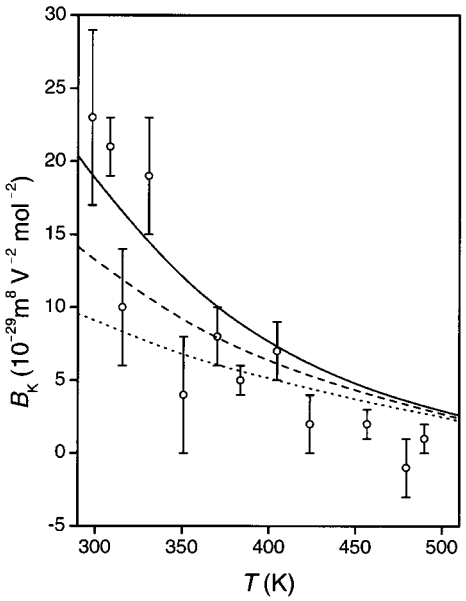

Figure 3. Comparison of calculated and observed temperature dependence of B_K of CH_3COCH_3. Force constants and shape factors (R_0, ϵ/k, D_1, D_2) for the calculated curves are the following: solid curve (0.46 nm, 380 K, 0.2058, 0.2267); dashed curve (0.47 nm, 360 K, 0.2106, 0.2319); dotted curve (0.48 nm, 380 K, 0.2094, 0.2306).

species. Unfortunately, the precision of the present experimental values of the second Kerr virial coefficient is insufficient to allow a definitive set of values of R_0, ϵ/k, D_1, and D_2 to be specified, and complementary investigations of the analogous second dielectric, refractivity, and light-scattering virial coefficients will be awaited with interest.

Summary

The evaluation of the free-molecule principal polarizabilities of asymmetric tops has long been an important goal but, after more than 70 years,[25] the necessary experimental data are available for only a limited number of relatively small molecules. There are good reasons why this is so, but these will not be discussed here. In the present study, the usefulness of the vapor-phase electrooptical Kerr effect, in conjunction with the mean polarizability and the Rayleigh depolarization ratio, has again been demonstrated and, as a result of a judicious combination of theory and experiment, the polarizabilities of HCHO, CH_3CHO, and CH_3COCH_3 can now be said to be reliably known. As well, it has been shown that the observed pressure dependence of the Kerr effect of CH_3COCH_3 is consistent with a statistical-mechanical theory based on the dipole-induced dipole model of intermolecular collisions.

Acknowledgment. Financial support from the National Research Foundation (to V.W.C.), an Australian Postgraduate Award (to R.I.K.), and the assistance of Dr. I. R. Gentle and Dr. D. W. Lamb with the measurements of the Kerr and Cotton−Mouton effects of acetone are gratefully acknowledged.

References and Notes

(1) (a) University of Natal. (b) University of New England.

(2) Buckingham, A. D. *Adv. Chem. Phys.* **1967**, *12*, 107−142.

(3) Bogaard, M. P.; Orr, B. J. *MTP Int. Rev. Sci.: Phys. Chem., Ser. 2* **1975**, *2*, 149−194.

(4) Buckingham, A. D. Basic Theory of Intermolecular Forces: Applications to Small Molecules. In *Perspectives in Quantum Chemistry and Biochemistry*; Pullman, B., Ed.; Wiley-Interscience: Chichester, 1978; Vol. 2, pp 1−67.

(5) Murphy, W. F. *J. Chem. Phys.* **1977**, *67*, 5877−5882.

(6) Murphy, W. F. *J. Raman Spectrosc.* **1981**, *11*, 339−345.

(7) Gentle, I. R.; Laver, D. R.; Ritchie, G. L. D. *J. Phys. Chem.* **1990**, *94*, 3434−3437.

(8) Tammer, R.; Hüttner, W. H. *Mol. Phys.* **1994**, *83*, 579−590.

(9) Coonan, M. H.; Ritchie, G. L. D. *Chem. Phys. Lett.* **1998**, *293*, 197−201.

(10) (a) Rice, J. E.; Amos, R. D.; Colwell, S. M.; Handy, N. C.; Sanz, J. *J. Chem. Phys.* **1990**, *93*, 8828−8839. (b) Rice, J. E.; Handy, N. C. *J. Chem. Phys.* **1991**, *94*, 4959−4971.

(11) Couling, V. W.; Graham, C. *Mol. Phys.* **1998**, *93*, 31−47.

(12) Couling, V. W.; Graham, C. *Mol. Phys.* **2000**, *98*, 135−138.

(13) Buckingham, A. D.; Galwas, P. A.; Liu Fan-Chen *J. Mol. Struct.* **1983**, *100*, 3−12.

(14) Bridge, N. J.; Buckingham, A. D. *Proc. R. Soc. London, Ser. A* **1966**, *295*, 334−349.

(15) Otterbein, G. *Phys. Z.* **1934**, *35*, 249−265.

(16) (a) Buckingham, A. D.; Pople, J. A. *Proc. Phys. Soc. A* **1955**, *68*, 905−909. (b) Buckingham, A. D. *Proc. Phys. Soc. A* **1955**, *68*, 910−919.

(17) Buckingham, A. D.; Orr, B. J. *Trans. Faraday Soc.* **1969**, *65*, 673−681.

(18) Perrin, D. D.; Armarego, W. L. F.; Perrin, D. R. *Purification of Laboratory Chemicals*, 2nd ed.; Pergamon: Oxford, U.K., 1980.

(19) Keir, R. I.; Ritchie, G. L. D. *Chem. Phys. Lett.* **1998**, *290*, 409−414.

(20) Bogaard, M. P.; Buckingham, A. D.; Pierens, R. K.; White, A. H. *J. Chem. Soc., Faraday Trans. 1* **1978**, *74*, 3008−3015.

(21) (a) Gentle, I. R.; Laver, D. R..; Ritchie, G. L. D. *J. Phys. Chem.* **1989**, *93*, 3035−3038. (b) Gentle, I. R.; Ritchie, G. L. D. *J. Phys. Chem.* **1989**, *93*, 7740−7744.

(22) Buckingham, A. D.; Orr, B. J. *Proc. R. Soc. London, Ser. A* **1968**, *305*, 259−269.

(23) Buckingham, A. D.; Le Fèvre, R. J. W. *J. Chem. Soc.* **1953**, 4169−4170.

(24) Dymond, J. H.; Smith, E. B. *The Virial Coefficients of Pure Gases and Mixtures*; Clarendon Press: Oxford, U.K., 1980.

(25) Stuart, H. A. *Z. Phys.* **1930**, *63*, 533−557.

(26) Lamb, D. W.; Ritchie, G. L. D. Unpublished data. See ref 9 for an example of the use of the temperature dependence of the Cotton−Mouton effect as the source of an independent equation in the molecular polarizabilities of an asymmetric top and a summary of the relevant equations.

(27) Oldag, F.; Sutter, D. H. *Z. Naturforsch.* **1992**, *47a*, 527−532.